Ultrafast responses of uniform- and gradient-doped GaAs photocathodes: from theory to experiment

Zhou, Rui, Jani, Hemang, Zhang, Yijun, Qian, Yunsheng, Duan, Lingze

Rui Zhou, Hemang Jani, Yijun Zhang, Yunsheng Qian, Lingze Duan, "Ultrafast responses of uniform- and gradient-doped GaAs photocathodes: from theory to experiment," Proc. SPIE 11999, Ultrafast Phenomena and Nanophotonics XXVI, 119990C (7 March 2022); doi: 10.1117/12.2607632

SPIE.

Event: SPIE OPTO, 2022, San Francisco, California, United States

Ultrafast responses of uniform- and gradient-doped GaAs photocathodes – from theory to experiment

Rui Zhou[a], Hemang Jani[a], Yijun Zhang[b], Yunsheng Qian[b], and Lingze Duan[a]

[a]Department of Physics and Astronomy, The University of Alabama in Huntsville, 301 Sparkman Drive, Huntsville, AL 35899, USA
[b]School of Electronic and Optical Engineering, Nanjing University of Science and Technology, Nanjing 210094, China

ABSTRACT

Semiconductor photocathodes with gradient-doping structures have attracted lots of interest in recent years because of their improved performances, such as higher quantum efficiency and longer diffusion length, over uniform-doped devices. It has been suggested that such improvement is due to the built-in electric field generated by the gradient of the doping concentration in the active layer. Under this built-in field, photoelectrons migrate toward the device surface via both diffusion and directional drift. While some past reports have studied and compared the photoelectron behaviors in uniform- and gradient-doped GaAs photocathodes, most of them are based on steady-state measurement and analysis. There has been little prior work focusing on dynamic responses. In this presentation, we report a comparative study of the ultrafast response of a uniform-doped and a gradient-doped GaAs photocathode, both theoretically and experimentally. We first develop a generalized diffusion-drift model, which adds a built-in electric field to a carrier diffusion model to incorporate the carrier drift. Then the theoretical model is used to predict the ultrafast transient behaviors of photoelectrons in *both* uniform- and gradient-doped photocathodes. Finally, the transient reflectivity of the photocathode devices is experimentally measured using pump-probe reflectometry (PPR), and the results are compared to the theoretical predictions. These comparisons indicate that the theoretical model is able to offer an appropriate physical picture of carrier transportation inside GaAs photocathodes of different doping profiles. It also enables the evaluation of device parameters such as diffusion coefficient and carrier decay time via PPR measurement.

Keywords: Ultrafast spectroscopy, Few-cycle laser, Pump-probe reflectivity, Transient response, Carrier dynamics, GaAs photocathodes

1. INTRODUCTION

Negative-electron-affinity (NEA) III-V semiconductor photocathodes have been widely used in night vision, polarized-electron generation, ultraviolet detection, and photon-enhancement in emission tubes.[1–3]The term "Negative Electron Affinity" (NEA) is used to describe a class of GaAs photocathodes in which the vacuum potential energy is lower than the conduction band minimum in the bulk flat region whereby making the escape of photoexcited electrons easy into the vacuum and hence significantly improving the quantum efficiency (QE) of such devices. Owing to its tremendous applications for low-light application devices, these family of photocathodes have attracted a lot of interest over the last two decades due to their high quantum efficiency and low dark emission.[4,5]

Based on the widely accepted Spicer three step model,[6] photoemission from an NEA emitter is divided into a three-step process of (i) optical absorption, (ii) electron transport to the surface, and (iii) escape across the surface into vacuum. This model has not only provided a means of understanding the photoemission process in detail, but has also aided researchers for an efficient photocathode design. There are several reports in the past dedicated to the improvement of design and performance of III-V photocathodes for optimizing their quantum efficiencies and more stable device structures.[7–9] One important development in this direction is the

Further author information: (Send correspondence to Rui Zhou)
Rui Zhou: E-mail: rui.zhou@uah.edu

Ultrafast Phenomena and Nanophotonics XXVI, edited by Markus Betz, Abdulhakem Y. Elezzabi,
Proc. of SPIE Vol. 11999, 119990C · © 2022 SPIE · 0277-786X · doi: 10.1117/12.2607632

introduction of a gradient (or exponential) doping structure in the active layer of such devices. This method balances the requirements for long electron diffusion lengths and narrow surface band bending regions[10–13] and has shown promising results for enhancing the quantum efficiencies and spectral response in both transmission mode (t-mode) photocathodes[14] and reflection mode (r-mode) photocathodes.[15] It has been suggested that such enhancement is due to the built-in electric field caused by the doping concentration gradient in the active layer of the devices. As a result, in such photocathodes, the photoelectrons can be transported toward the surface through both diffusion and directional drift.[11,12] In prior studies, theoretical models have been developed to describe the impacts of drift on key specifications of NEA GaAs photocathodes, such as diffusion length and QE.[12,16] However, all the existing theories are based on steady-state analysis, which assumes the photocathode is under a constant illumination of light.

Meanwhile, an important application of III-V photocathodes is the generation of electron bunches using pulsed lasers,[17–20] which has also been utilized to investigate the carrier-diffusion dynamics in GaAs photocathodes.[17,18,21] The existing steady-state theories are incapable of explaining photoelectron transportation in these cases, therefore a time-dependent dynamic model has become necessary. Previously, we have developed a diffusion model to explain the behaviors of the photoelectrons in a *uniform-doped* GaAs photocathode following the photoexcitation by a femtosecond laser pulse,[21,22] and we have also reported direct experimental evidence of drift-assisted carrier transportation in gradient-doped devices.[23] In this paper, we generalize the theory to incorporate the carrier drift by adding a built-in electric field to the carrier diffusion model. We further verify the model by comparing it with experimental results from femtosecond pump-probe reflectometry (PPR) measurements.[21,24] Comparisons are made for both uniform-doped and gradient-doped GaAs photocathode devices. Great experiment-theory agreements are realized, demonstrating the effectiveness of the theory in explaining the photoelectron dynamics in real devices.

2. THEORETICAL MODEL

In a gradient-doped semiconductor photocathode, the p-type doping concentration varies exponentially with depth (such a device is also known as exponential-doped). Mathematically, this depth-dependent doping profile can be written as

$$N_d(x) = N_{d0}\exp(Ax), \tag{1}$$

where N_{d0} is the doping concentration on the surface of the photocathode, A is the gradient doping coefficient, and x is the depth from the surface. The doping gradient creates a *constant* electric field normally pointing into the device with a magnitude of

$$E = -\frac{d}{dx}\left(\frac{k_0T}{q}\ln\frac{N_{d0}}{N_d(x)}\right) = \frac{k_0TA}{q}, \tag{2}$$

where k_0 is the Boltzmann constant, T is temperature, and q is the elementary charge.

Our theoretical electron transportation model for the gradient-doped GaAs photocathods is built upon a two-layer model previously developed for the uniform-doped devices.[21] In the two-layer model, the heavily p-doped GaAs layer is divided into two distinct sublayers: an active layer (AL), where most of the photoelectron generation and transportation take place, and a very thin band-bending region (BBR) near the surface, where the photoelectrons accumulate and decay. Separate analyses will be applied to AL and BBR respectively based on the different electron behaviors inside them. Fig. 1 illustrates the band scheme, the coordinate system, the definitions of the sublayers, as well as the doping configuration in the active layer (darker pattern indicates higher doping concentration).

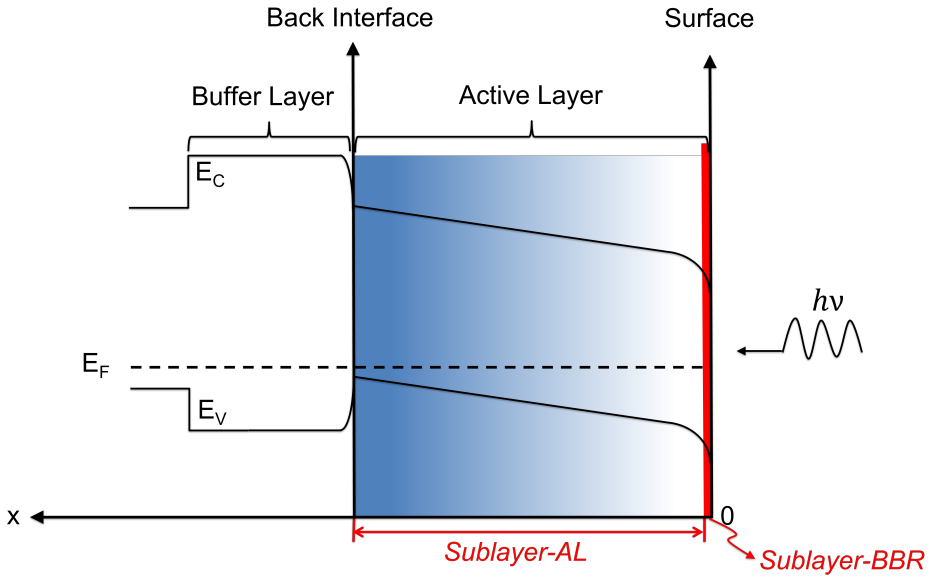

Figure 1. The band scheme of a typical gradient-doped GaAs photocathode with illustration of the two sublayers: the active layer (AL) and the band-bending region (BBR).

2.1 The Active Layer (AL)

The electron concentration $n(x,t)$ inside the AL follows the 1D continuity equation, which can be derived from the general continuity equation and written as:

$$\frac{\partial n(x,t)}{\partial t} = D\frac{\partial^2 n(x,t)}{\partial x^2} + \mu_n|E|\frac{\partial n(x,t)}{\partial x} + \mu_n\, n(x,t)\frac{\partial |E|}{\partial x} - \frac{n(x,t)}{\tau_m} + g_n, \tag{3}$$

where D is the diffusion coefficient, μ_n is the electron mobility, E is the doping-induced built-in electric field given by Eq. (2), τ_m is the mean electron lifetime, and g_n is the rate of electron generation caused by all external factors.

As pointed out earlier, the built-in electric field is constant and independent of location in a gradient doping structure. Thus, the term $\partial|E|/\partial x = 0$ in Eq. (3). Secondly, based on our two-layer model, we can treat the AL as decay-free and lump all electron decay into the BBR, which eliminates the term $n(x,t)/\tau_m$ in Eq. (3). Finally, photoelectron generation by a femtosecond pulse is considered as an instantaneous process, so g_n can be merged into the initial condition. After these simplifications, the continuity equation becomes

$$\frac{\partial n(x,t)}{\partial t} = D\frac{\partial^2 n(x,t)}{\partial x^2} + v_d\frac{\partial n(x,t)}{\partial x}, \tag{4}$$

where the drift velocity v_d is introduced and defined as $v_d = \mu_n|E|$. By inserting the built-in electric field given in Eq. (2) and the Einstein relation $D/\mu_n = k_0T/q$, v_d can be linked to the diffusion coefficient D and the gradient doping coefficient A as $v_d = DA$. The initial condition is $n(x,0) = n_0e^{-\alpha x}$, where α is the absorption coefficient in the AL and n_0 is a scale factor for the electron population density. For simplicity, n_0 has been chosen in our model to make $\int_0^d n_0\, e^{-\alpha x}dx = 1$, where d is the thickness of the AL. We further assume the BBR acts as an electron "sink" and the back interface of the AL is an impenetrable "wall". This leads to a Dirichlet boundary condition $n(0,t) = 0$ on the AL-BBR interface and a Neumann boundary condition $\partial n(x=d,t)/\partial x = 0$ on the back interface.

Eq. (4) can be then solved with the initial condition and the boundary conditions, and the general solution can be written as

$$n(x,t) = 2n_0\, e^{-\gamma x} \sum_{i=1}^{\infty} b_i \sin(a_i x)\, e^{-\beta_i D t}, \tag{5}$$

where β_i and γ have been introduced to simplify the expression and are defined as

$$\beta_i = \frac{A^2}{4} + {a_i}^2, \quad \gamma = \frac{A}{2}. \tag{6}$$

The expansion coefficients a_i and b_i are ruled by the boundary conditions and the initial condition, respectively. Applying the Neumann boundary condition at the back interface to the general solution (5) results in a transcendental equation

$$\tan(a_i d) = \frac{2}{Ad}(a_i d). \tag{7}$$

In general, Eq. (7) has to be solved numerically, and a set of discrete solutions for a_i can be found and used to obtain the general solution.[25] However, in the special case of a small doping gradient, an approximate analytical solution can be developed. This can be done by converting Eq. (7) into a set of parametric equations with $u(y) = \tan(y)$ and $v(y) = \frac{2}{Ad}y$, where $y = a_i d$, and seeking the intersections between $u(y)$ and $v(y)$. When the slope $\frac{2}{Ad}$ in $v(y)$ is large, or in other words, when the product of Ad is small, the intersections are very close to $y = (i - \frac{1}{2})\pi$, where i is a positive integer. This leads to a set of approximate solutions for a_i

$$a_i = \frac{2i-1}{2d}\pi, \; i = 1, 2, 3 \cdots . \tag{8}$$

Further applying the initial condition $n(x,0) = n_0 e^{-\alpha x}$ to Eq. (5) and completing the Fourier expansion, the coefficient b_i is found to be

$$b_i = \frac{a_i + (-1)^i(\alpha - \gamma)\, e^{-(\alpha-\gamma)d}}{d[(\alpha-\gamma)^2 + {a_i}^2]}. \tag{9}$$

2.2 The Band-Bending Region (BBR)

In the BBR, the governing equation is the modified continuity equation

$$\frac{\partial N(t)}{\partial t} = J(t) - \Gamma N(t), \tag{10}$$

where $N(t)$ is the total electron population in the BBR, Γ is the electron decay rate, which includes all the effects that lead to the reduction of the photoelectron population. $J(t)$ is the AL-to-BBR injection flux, which can be found by

$$J(t) = \frac{d}{dt}\left[1 - \int_0^d n(x,t)dx\right]. \tag{11}$$

With the help of Eq. (8) and (9), the differential equation (10) can be solved and the analytical expression for the total electron population in the BBR can be simplified as

$$N(t) = 2n_0 D \sum_{i=1}^{\infty} b_i \frac{a_i + (-1)^i \gamma\, e^{-\gamma d}}{\gamma^2 + a_i^2} \frac{\beta_i}{\Gamma - \beta_i D}\left(e^{-\beta_i D t} - e^{-\Gamma t}\right), \tag{12}$$

where the coefficients a_i and b_i keep the same expressions as given in Eq. (8) and (9).

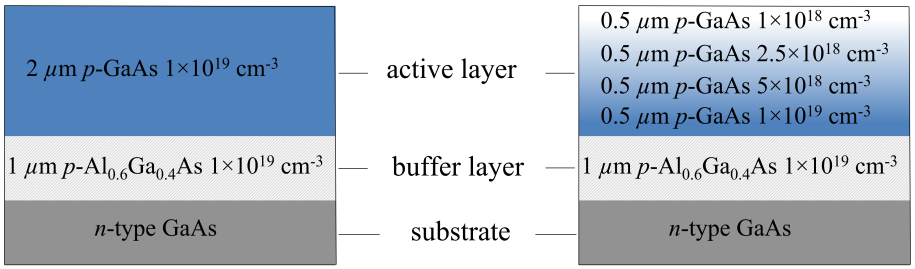

Figure 2. The doping structure of the uniform-doped (left) and gradient-doped (right) GaAs photocathode.

Thus the theoretical model for the photoelectron transportation in a gradient-doped, with small doping coefficient, GaAs photocathode is fully established. The beauty of this model is that it can as well represent the uniform-doping structure. By setting the gradient coefficient $A = 0$, and simplify the coefficients β_i, γ, a_i and b_i accordingly, the final result agrees with our previously reported result based on a diffusion-only model.[21] Therefore, we can confidently say that this theoretical model is capable to explain the electron transportation dynamics in both gradient- and uniform-doped GaAs photocathodes.

3. THEORY-EXPERIMENT COMPARISONS

The above model can be compared with experiment by substituting device parameters into Eq. (12). According to the well-known Drude theory,[26,27] the change of the surface reflectivity of the a semiconductor is proportional to the area density of the electrons accumulated on the surface of the device,[21] which is directly correlated to the total electron population $N(t)$ in our 1D model as mentioned earlier. Prior results have shown that multiple decay channels may exist in such devices.[21] As a result, we have incorporated a *bi-exponential* decay model in our numerical calculation.[21] In specific, we consider the total electron population accumulated in the BBR as the sum of two independent decay processes. Since the free-electron population is in principle proportional to the transient reflectivity $\Delta R(t)$, the overall transient behavior of $\Delta R(t)$ hence can be modeled by

$$\Delta R(t) \propto N(t) = C_1 N_{\Gamma 1}(t) + C_2 N_{\Gamma 2}(t), \tag{13}$$

where $N_{\Gamma 1}(t)$ and $N_{\Gamma 2}(t)$ are the populations of the two electron groups with the decay rates Γ_1 and Γ_2, respectively. C_1 and C_2 represent the partition of the total electron population and satisfy $C_1 + C_2 = 1$.

Experimental measurement of $\Delta R(t)$ has been performed using our home-built PPR system,[21,24] which is based on a 6.5-fs Ti:sapphire laser operating at a center wavelength of 800 nm, with an average power of 500 mW and a repetition rate of 83 MHz. Two samples of GaAs photocathodes have been tested, including one uniform-doped and one gradient-doped device. Both of them are fabricated with molecular-beam epitaxy (MBE) method. The doping structures are illustrated in Fig. 2. They both have a 1-μm buffer layer of p-$Al_{0.6}Ga_{0.4}As$ with a doping concentration of 1×10^{19} cm^{-3} directly grown on the n-type GaAs substrate, and a 2-μm active layer made of p-doped GaAs. For the unifom-doped device, the active layer has a uniform doping concentration of 1×10^{19} cm^{-3}. Whereas for the gradient-doped sample, the doping concentration varies from 1×10^{19} cm^{-3} near the buffer layer to 1×10^{18} cm^{-3} on the surface.

Fig. 3(a) and (b) show the PPR-measured transient reflectivity for the uniform- and gradient-doped photocathode device, respectively. In both cases, $\Delta R(t)$ experiences an initial sharp rise followed by a decay process. Furthermore, the decay, in both cases, includes a quick drop immediately following the peak and a relatively long, slowly-decreasing tail, indicating the existence of two decay mechanisms with markedly different decay rates. Using the bi-exponential model given by Eq. (13), excellent agreements between theory and experiment are obtained for both devices, as shown in Fig. 3. The corresponding fitting parameters are given in Table 1. These parameters suggest that the fast decay process has a decay time of about 1-2 ps, whereas the slow decay process is typically tens of times slower. In both devices, over 90% of the photoelectrons are lost during the

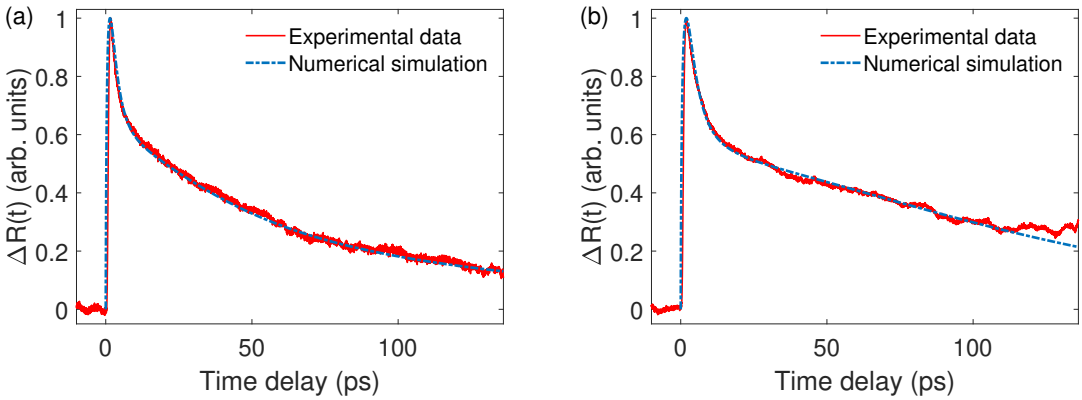

Figure 3. Comparisons between the numerical simulation and experimental data for the (a) uniform-doped and (b) gradient-doped photocathode samples.

Table 1. Device parameters used in theoretical model in Fig. 3

Sample Type	D (cm^2/s)	v_d (cm/s)	C_1	$\tau_1 = 1/\Gamma_1$ (ps)	C_2	$\tau_2 = 1/\Gamma_2$ (ps)
(a) uniform-doped	120	0	0.9	1.3	0.1	30
(b) gradient-doped	160	1.84×10^6	0.916	1.8	0.084	70

fast decay process. Although the exact underlying physical mechanisms are not clear solely based on these results, the fast and the slow decay times appear to match the typical time scales of surface recombination and photoemission, respectively, according to prior studies on similar GaAs photocathodes.[18,20,21,28]

It should be pointed out here that the above comparisons are intended to validate the theoretical model rather than to compare the performances of the photocathodes themselves. Therefore, *normalized* transient reflectivity traces are used and the actual scales of the measured PPR responses are neglected in the current study.

4. CONCLUSION

In conclusion, we report a general theoretical model describing photoelectron transportation dynamics in GaAs photocathodes. In this model, a generalized diffusion equation incorporating directional drift caused by doping gradient has been developed. Time-dependent electron concentration distribution is obtained, under the small doping gradient assumption, by solving this generalized diffusion equation. The transient reflectivity behaviors of both uniform-doped and gradient-doped GaAs photocathodes are characterized using femtosecond pump-probe reflectometry. Our results show excellent agreements between the numerical predictions and the experimental measurements whereby confirming the effectiveness of our model in explaining experimental observations for both uniform- and gradient-doped devices. Moreover, with the theoretical model, the important characteristic parameters of the devices, such as the diffusion coefficient, the drift velocity and the decay time, can be evaluated quantitatively.

ACKNOWLEDGMENTS

This work was funded in part by the National Science Foundation (NSF) under Grants ECCS-1254902 and ECCS-1606836. The authors gratefully acknowledge the support by Dr. Liang Chen and Dr. Shuqin Zhang of the China Jiliang University.

REFERENCES

[1] Bakin, V. V., Pakhnevich, A. A., Zhuravlev, A. G., Shornikov, A. N., Tereshechenko, O. E., Alperovich, V. L., Scheibler, H. E., and Terekhov, A. S., "Semiconductor surfaces with negative electron affinity," *e-Journal of Surface Science and Nanotechnology* **5**, 80–88 (2007).

[2] La Rue, R. A., Costello, K. A., Davis, C., Edgecumbe, J. P., and Aebi, V. W., "Photon counting III-V hybrid photomultipliers using transmission mode photocathodes," *IEEE Transactions on Electron Devices* **44**(4), 672–678 (1997).

[3] Liu, Z., Sun, Y., Peterson, S., and Pianetta, P., "Photoemission study of Cs–NF 3 activated GaAs (100) negative electron affinity photocathodes," *Applied Physics Letters* **92**(24), 241107 (2008).

[4] Karkare, S., Boulet, L., Cultrera, L., Dunham, B., Liu, X., Schaff, W., and Bazarov, I., "Ultrabright and ultrafast III–V semiconductor photocathodes," *Physical review letters* **112**(9), 097601 (2014).

[5] Chen, X., Tang, G., Wang, D., and Xu, P., "High quantum efficiency transmission-mode GaAlAs photocathode with a nanoscale surface structure," *Optical Materials Express* **8**(10), 3155–3162 (2018).

[6] Spicer, W. E. and Herrera-Gomez, A., "Modern theory and applications of photocathodes," **2022**, 18, International Society for Optics and Photonics (oct 1993).

[7] Bell, R. L. and Spicer, W. E., "3–5 Compound Photocathodes: A New Family of Photoemitters with Greatly Improved Performance," *Proceedings of the IEEE* **58**(11), 1788–1802 (1970).

[8] Olsen, G. H., Szostak, D. J., Zamerowski, T. J., and Ettenberg, M., "High-performance GaAs photocathodes," *Journal of Applied Physics* **48**(3), 1007–1008 (1977).

[9] Gregory, P. E., Escher, J. S., Saxena, R. R., and Hyder, S. B., "Field-assisted photoemission to 2.1 microns from a Ag/ p -In $_{0.77}$Ga$_{0.23}$As photocathode," *Applied Physics Letters* **36**, 639–640 (apr 1980).

[10] Zou, J. and Chang II, B., "Gradient-doping negative electron affinity GaAs photocathodes," *Optical Engineering* **45**(5), 054001 (2006).

[11] Yang, Z., Chang, B., Zou, J., Qiao, J., Gao, P., Zeng, Y., and Li, H., "Comparison between gradient-doping GaAs photocathode and uniform-doping GaAs photocathode," *Applied Optics* **46**(28), 7035–7039 (2007).

[12] Niu, J., Zhang, Y., Chang, B., Yang, Z., and Xiong, Y., "Influence of exponential doping structure on the performance of GaAs photocathodes," *Applied optics* **48**(29), 5445–5450 (2009).

[13] Zhang, Y., Zhao, J., Zou, J., Niu, J., Chen, X., and Chang, B., "The high quantum efficiency of exponential-doping AlGaAs/GaAs photocathodes grown by metalorganic chemical vapor deposition," *Chinese Physics Letters* **30**(4), 044205 (2013).

[14] Zhang, Y., Niu, J., Zhao, J., Zou, J., Chang, B., Shi, F., and Cheng, H., "Influence of exponential-doping structure on photoemission capability of transmission-mode GaAs photocathodes," *Journal of Applied Physics* **108**(9), 093108 (2010).

[15] Zhang, Y., Zou, J., Niu, J., Zhao, J., and Chang, B., "Photoemission characteristics of different-structure reflection-mode GaAs photocathodes," *Journal of Applied Physics* **110**(6), 063113 (2011).

[16] Cai, Z., Yang, W., Tang, W., and Hou, X., "Numerical analysis of temporal response of a large exponential-doping transmission-mode GaAs photocathode," *Materials science in semiconductor processing* **16**(2), 238–244 (2013).

[17] Hartmann, P., Bermuth, J., v. Harrach, D., Hoffmann, J., Köbis, S., Reichert, E., Aulenbacher, K., Schuler, J., and Steigerwald, M., "A diffusion model for picosecond electron bunches from negative electron affinity GaAs photocathodes," *Journal of applied physics* **86**(4), 2245–2249 (1999).

[18] Honda, Y., Matsuba, S., Jin, X., Miyajima, T., Yamamoto, M., Uchiyama, T., Kuwahara, M., and Takeda, Y., "Temporal response measurements of GaAs-based photocathodes," *Japanese Journal of Applied Physics* **52**(8R), 086401 (2013).

[19] Jin, X., Matsuba, S., Honda, Y., Miyajima, T., Yamamoto, M., Utiyama, T., and Takeda, Y., "Picosecond electron bunches from GaAs/GaAsP strained superlattice photocathode," *Ultramicroscopy* **130**, 44–48 (2013).

[20] Aulenbacher, K., Schuler, J., Harrach, D. v., Reichert, E., Röthgen, J., Subashev, A., Tioukine, V., and Yashin, Y., "Pulse response of thin III/V semiconductor photocathodes," *Journal of applied physics* **92**(12), 7536–7543 (2002).

[21] Jani, H., Chen, L., and Duan, L., "Pre-emission study of photoelectron dynamics in a GaAs/AlGaAs photocathode," *IEEE Journal of Quantum Electronics* **56**(1), 1–8 (2019).

[22] Jani, H., Zhou, R., Zhang, Y., Qian, Y., and Duan, L., "Pump-probe study of ultrafast response of GaAs photocathodes grown by MOCVD and MBE," in [*Ultrafast Phenomena and Nanophotonics XXIV*], **11278**, 112780R, International Society for Optics and Photonics (2020).

[23] Zhou, R., Jani, H., and Duan, L., "Direct Evidence of Drift-Assisted Carrier Transportation in a Gradient-Doped GaAs Photocathode," in [*CLEO: Applications and Technology*], JW2F–35, Optical Society of America (2020).

[24] Jani, H. and Duan, L., "Time-Frequency Spectroscopy of GaAs Transient Dispersion Using Few-Cycle Pump-Probe Reflectometry," *Physical Review Applied* **13**(5), 054010 (2020).

[25] Zhou, R., Jani, H., Zhang, Y., Qian, Y., and Duan, L., "Photoelectron transportation dynamics in GaAs photocathodes," *Journal of Applied Physics* **130**(11), 113101 (2021).

[26] Tanaka, T., Harata, A., and Sawada, T., "Subpicosecond surface-restricted carrier and thermal dynamics by transient reflectivity measurements," *Journal of applied physics* **82**(8), 4033–4038 (1997).

[27] Glezer, E., Siegal, Y., Huang, L., and Mazur, E., "Laser-induced band-gap collapse in GaAs," *Physical Review B* **51**(11), 6959 (1995).

[28] Hang, S., Liu, Y., Li, H., Tang, X., and Chen, D., "Temporal characteristic analysis of laser-modulated pulsed X-ray source for space X-ray communication," *Nuclear Instruments and Methods in Physics Research Section A: Accelerators, Spectrometers, Detectors and Associated Equipment* **887**, 18–26 (2018).